


 Cite this: *RSC Adv.*, 2022, 12, 29535

Enzyme-linked aptamer-based sandwich assay (ELASA) for detecting *Plasmodium falciparum* lactate dehydrogenase, a malarial biomarker

 Yeon-Jun Kim ^a and Jae-Won Choi ^{*ab}

Herein, we report a sensitive and selective enzyme-linked aptamer-based sandwich assay (ELASA) to detect *Plasmodium falciparum* lactate dehydrogenase (*PfLDH*), which is an attractive biomarker for malaria diagnosis and antimalarial medication. We performed the sandwich assay with a single aptamer sequence, called 2008s, owing to the structural properties of the *PfLDH* tetramer instead of using a conventional sandwich assay with two different aptamers (or antibodies) for capturing and probing a target molecule. First, the biotinylated *PfLDH* aptamer was linked with immobilized streptavidin on a microwell plate for binding flexibility, and then *PfLDH* was bound to the aptamer. Next, a horseradish peroxidase-conjugated aptamer of the same sequence was used to analyze *PfLDH* quantitatively. Using this approach, the limit of detection (LOD) of *PfLDH* with the naked eye was 100 ng mL⁻¹, and the LOD and limit of quantification from the absorbance measurements were 34.9 ng mL⁻¹ and 95.5 ng mL⁻¹, respectively, based on *PfLDH* spiked blood samples. Our proposed method selectively binds *PfLDH*, not human lactate dehydrogenase. Therefore, this method may be a valuable tool for diagnosing, monitoring, and quarantining malaria cases easily and rapidly.

 Received 20th June 2022
 Accepted 8th October 2022

DOI: 10.1039/d2ra03796c

rsc.li/rsc-advances

Introduction

Malaria is an infectious disease caused by parasitic protozoans of the *Plasmodium* species, often occurring in tropical or semi-tropical regions and commonly transmitted to humans by female mosquitoes.^{1–3} Malaria symptoms appear within a few days of being bitten by a mosquito, including fever, fatigue, sweating, nausea, vomiting, diarrhea, and headache.³ Even though anti-malarial medications can cure malaria, The World Malaria Report 2021, published by the World Health Organization, reported over 241 million malaria patients and approximately 627 000 malaria-related fatalities in 85 malaria-endemic countries.¹ Therefore, quick diagnosis with an accurate and straightforward platform is essential for obtaining proper medical treatment.

Currently, a microscopic examination,^{4–6} polymerase chain reaction (PCR),^{7–9} and a rapid diagnostic test (RDT)^{10–12} are widely utilized for diagnosing malaria. A peripheral blood smear test with a microscopic examination is the most accurate method for confirming the malaria parasites.¹³ Although the technique is old, it remains the most widely used due to its high accuracy and positioning as a gold standard. However, it requires sophisticated equipment, experienced experts, and several days for high-accuracy analyses. Generally, a PCR assay is employed to detect parasitic DNA with high sensitivity, but its

complexity and cost are barriers for general use. PCR also requires equipped laboratory facilities and has difficulties detecting cases of plasmodial genotypic variants.⁷ RDT diagnoses malaria quickly and easily, but its sensitivity and specificity are manufacturer-dependent, quantitative analysis is impossible, and early diagnosis is difficult.

Enzyme-linked immunosorbent assay (ELISA) is the most actively used format for target molecule detection in liquid or wet samples because of its robust and accurate properties.^{14–16} ELISAs use antibodies and colorimetric substrates to identify a specific antigen in a sample. Malaria diagnosis is based on various protein biomarkers (or antigens), such as plasmodial lactate dehydrogenase (LDH),^{10,11,16} histidine-rich protein II,^{12,17,18} aldolase,¹⁹ and glutamate dehydrogenase.²⁰ Among these biomarkers, plasmodial LDH (pLDH) is an attractive target for malaria diagnosis and antimalarial drug design since it produces plasmodial ATP in human red blood cells and has unique amino acids at the active site and a well-understood three-dimensional structure.^{21–23} Some results have reported successful ELISA-based malaria diagnosis using antibodies against *Plasmodium* spp. LDH.^{16,24} However, the ELISA method is an antibody-based detection format; thus, monoclonal or polyclonal antibodies against a specific antigen are necessary. In addition, this format requires sacrificing laboratory animals, such as mice and rabbits, and takes several months to produce the same antibodies. Recently, mass antibody production has trended toward a cell culture system using a bioreactor, eliminating the need for animals. However, this is also not ideal

^aDepartment of Biomedical Science, Cheongju University, Cheongju 28160, Republic of Korea. E-mail: jwchoi0211@gmail.com; jwchoi@cju.ac.kr

^bDepartment of Bioindustrial Engineering, Cheongju 28503, Republic of Korea



since it requires many additional elements (*e.g.*, medium, antibiotics, and serum), takes time, and can be costly.

An aptamer is an oligonucleic acid that can specifically bind from small molecules such as metal ions and chemicals to large molecules such as proteins. In recent, several aptamers capable of binding to pLDH have been developed by the systematic evolution of ligands by exponential enrichment (*i.e.*, SELEX) for diagnosing malaria.^{21,25,26} Aptamers can be used to develop aptasensors for diagnosing malaria because they are easily synthesizable and have high specificity and thermal stability. Above all, unlike antibodies, aptamers can be mass-produced by chemical synthesis without animals or bioreactors.

Of the four malaria-causing *Plasmodium* spp. (*P. falciparum*, *P. vivax*, *P. malariae*, and *P. ovale*), *P. falciparum* triggers the version of malaria that is most often fatal and medically severe; this species causes most malarial deaths.^{1,3} Several aptamers specifically bind to *P. falciparum* lactate dehydrogenase (*Pf*LDH), but the 2008s aptamer is used the most for detecting *Pf*LDH because it has excellent and stable binding.^{21,27–29} Herein, we aimed to develop a simple yet effective aptamer-based *Pf*LDH detection method and report an enzyme-linked aptamer-based sandwich assay (ELASA) for rapid and sensitive detection of *Pf*LDH using the 2008s aptamer.

Experimental

Reagents and materials

Streptavidin from *Streptomyces avidinii*, horseradish peroxidase (HRP), lysozyme, imidazole, Tris powder, 1-fluoro-2,4-dinitrobenzene (FDNB), phenylmethylsulfonyl fluoride (PMSF), sodium bicarbonate, sodium carbonate, sodium phosphate, sodium periodate, and sodium borohydride were purchased from Sigma-Aldrich (St. Louis, MO, USA). Ampicillin and isopropyl β -D-1-thiogalactopyranoside (IPTG) were purchased from LPS Solution (Daejeon, Republic of Korea). All enzymes for plasmid construction were purchased from Enzygnomics (Daejeon, Republic of Korea). Pyridoxal phosphate and phosphate buffered saline (pH 7.4) were obtained from AMRESCO (Solon, OH, USA), and ethylene glycol was purchased from Junsei Chemical (Tokyo, Japan). Bovine serum albumin (BSA) was purchased from Roche (Basel, Switzerland). The bicinchoninic acid (BCA) protein assay kit was purchased from Thermo Fisher Scientific (Waltham, MA, USA). The 3,3',5,5'-tetramethylbenzidine (TMB) substrate was purchased from Kementec (Taastrup, Denmark). The single-stranded DNA aptamer that specifically binds to *Pf*LDH called '2008s' (5'-CTGGGCGGTAGAACCATAGTGACCCAGCCGTCTAC-3') was synthesized by Integrated DNA Technologies (Singapore, Republic of Singapore), and biotin or HRP was conjugated at 3'-end of aptamer, respectively. Human LDH (hLDH) was purchased from Abcam (Cambridge, UK).

*Pf*LDH expression and purification

A recombinant *Pf*LDH plasmid was constructed in pET-21a(+) and transformed into the BL21(DE3) strain of *Escherichia coli*. BL21(DE3) cells carrying pET-21a(+)-*Pf*LDH plasmids were

grown in lysogeny broth containing 50 $\mu\text{g mL}^{-1}$ of ampicillin by an OD₆₀₀ of 0.6. Recombinant *Pf*LDH proteins were induced with 1 mM IPTG at 20 °C for 16 h. Cells were harvested by centrifugation and then lysed using lysis buffer (20 mM Tris-Cl [pH 7.9], 5 mM imidazole, 500 mM NaCl, 1 mM PMSF, and 10 mg g⁻¹ [lysozyme/pellet]) by sonication. The lysates were centrifuged at 9000 rpm for 30 min at 4 °C. After centrifugation, the supernatant was loaded on a nickel-nitrilotriacetic acid (Ni-NTA) resin-packed column. The column was washed with washing buffer (20 mM Tris-Cl [pH 7.9], 40 mM imidazole, 500 mM NaCl, and 1 mM PMSF) and then eluted with elution buffer (20 mM Tris-Cl [pH 7.9], 500 mM imidazole, and 500 mM NaCl). The eluted *Pf*LDH proteins were dialyzed into a dialysis buffer containing 20 mM sodium phosphate, 500 mM NaCl, and 0.5 mM pyridoxal phosphate for 16 h at 4 °C. Finally, the *Pf*LDH concentration was confirmed by BCA protein assay kit.

Polyacrylamide gel electrophoresis (PAGE) of *Pf*LDH and hLDH

We performed PAGE to confirm the purification procedures of *Pf*LDH using a 12% polyacrylamide gel under reduced conditions containing sodium dodecyl sulfate (SDS) and β -mercaptoethanol (β -ME). PAGE was performed in both reduced and native conditions to identify purified *Pf*LDH and hLDH proteins. In the reduced condition, 4 \times reducing sample buffer containing 250 mM Tris-Cl (pH 6.8), 8% SDS, 40% glycerol, 8% β -ME, and 0.02% bromophenol blue was used. Then, SDS-PAGE was performed using a 15% polyacrylamide gel and 1 \times electrophoresis buffer containing 0.01% SDS. In the native condition, 4 \times native sample buffer containing 250 mM Tris-Cl (pH 6.8), 40% glycerol, and 0.02% bromophenol blue was used. Native PAGE was performed using a 10% polyacrylamide gel without SDS and 1 \times electrophoresis buffer without SDS.

HRP conjugation with *Pf*LDH

HRP (2.5 mg) was dissolved in 300 mM sodium carbonate buffer (pH 8.1). Then, FDNB was added to the HRP solution and incubated for 1 h at room temperature. Next, the solution was incubated with 80 mM of sodium periodate for 1 h at room temperature, and then 160 mM of ethylene glycol was added. After 1 h, the activated HRP solution was dialyzed into a 10 mM sodium bicarbonate buffer (pH 9.5) for 16 h at 4 °C. For *Pf*LDH, buffer exchange was performed by extensively dialyzing against the 10 mM sodium bicarbonate buffer (pH 9.5). Finally, 1 mg of *Pf*LDH was mixed with the HRP solution for 2 h at room temperature, and then this mixture was incubated with 5 mg mL⁻¹ of sodium borohydride for 2 h at 4 °C. The HRP-*Pf*LDH conjugates were purified *via* Ni-NTA resin and concentrated by a centrifugal filter unit from Merck Millipore (Billerica, MA, USA). The concentration of HRP-*Pf*LDH conjugates was determined by a NanoDrop 2000c spectrophotometer (Thermo Fisher Scientific).

Aptamer and *Pf*LDH binding affinity measurements

A 1 $\mu\text{g mL}^{-1}$ streptavidin solution was added to a 96-well microwell plate and incubated at 37 °C for 1 h. After streptavidin coating, all microwells were blocked with a blocking solution



containing 5% BSA, 5% sucrose, and 0.05% Tween-20 in phosphate-buffered saline (PBS) at 37 °C for 1 h. Then, the blocking solution was removed from the microwells, and the plate was dried at 37 °C for 1 h. Next, 10 nM of the biotin-conjugated *Pf*LDH aptamer was added to the streptavidin-coated microwell plate and incubated at 37 °C for 1 h. At this time, the aptamer was allowed to self-form a secondary structure through the cooling process at room temperature after denaturation at 90 °C for 30 seconds for structuration prior to being added into the microwell plate. Three different buffer conditions were used to determine the best structuration (buffer A: PBS, pH 7.4, buffer B: 25 mM Tris-Cl (pH 7.5), 100 mM NaCl, and 20 mM imidazole, and buffer C: 10 mM Tris-Cl (pH 7.4), 10 mM NaCl, and 0.2 mM MgCl₂). After incubation, all microwells were washed three times using 0.05% Tween-20 containing PBS (0.05% PBS-T). Finally, different concentrations of HRP-conjugated *Pf*LDH (serially diluted from 2 μM) were added to the microwells and incubated at 37 °C for 1 h. Finally, 100 μL of TMB substrate was added per microwell after washing for 15 min at room temperature to develop the colorimetric reaction. The reaction step was stopped *via* a 0.5 N H₂SO₄ solution, and the absorbance was measured at 450 nm using a Bio-Rad microplate reader (Hercules, CA, USA). The binding affinity between *Pf*LDH and the aptamer was calculated from the extracted absorbances per *Pf*LDH concentration. A microwell plate coated only with BSA without streptavidin was used as a negative control.

Aptamer and streptavidin binding affinity measurements

A 96-well plate was coated, blocked, and dried as described above. Next, different concentrations of structured HRP-conjugated *Pf*LDH aptamer (serially diluted from 1 μM) were added to the microwells and incubated at 37 °C for 1 h. After incubation, all microwells were washed three times using 0.05% PBS-T. The colorimetric reaction and spectrophotometric measurements were performed as described above.

Multiple sequence alignment of *Pf*LDH and hLDH amino acids

The homology of *Pf*LDH and hLDH amino acids was analyzed using the 'Align' mode in UniProt (<https://www.uniprot.org/align>). The UniProt entry ID corresponding to this experiment's *Pf*LDH amino acids sequence was Q76NM3 (entry name: Q76NM3_PLAF7, gene name: PF3D7_1324900), and the UniProt entry ID for hLDH was P00338 (entry name: LDHA_HUMAN, gene name: LDHA_PIG19).

*Pf*LDH and hLDH detection by ELISA

A 1 μM streptavidin solution was added to a 96-well microwell plate and incubated at 37 °C for 1 h. The 96-well microwell plate was blocked, and dried as described above. Then, 1 μM of structured biotin-conjugated *Pf*LDH aptamer was added to the streptavidin-coated microwell plate and incubated at 37 °C for 1 h. After incubation, all microwells were washed three times using washing buffer. Next, purified *Pf*LDH in buffer, hLDH in buffer, or spiked *Pf*LDH in mouse blood of various concentrations (0, 10⁻⁴, 10⁻³, 10⁻², 10⁻¹, 10⁰, 10¹, and 10² μg mL⁻¹) were loaded into the wells then incubated at 37 °C for 1 h. Then, after washing, 1 μM of structured HRP-conjugated *Pf*LDH aptamer was added to the microwell plate and incubated at 37 °C for 1 h. After washing, 100 μL of TMB substrate was added per microwell and then incubated at room temperature for 15 min. The reaction step was stopped using a 0.5 N H₂SO₄ solution, and the absorbance was measured at 450 nm using a microplate reader.

Results and discussion

*Pf*LDH and hLDH confirmation by PAGE

Before examining *Pf*LDH and the 2008s aptamer binding, we confirmed that purified recombinant *Pf*LDH was obtained by reduced and native PAGE analyses (Fig. 1); we found that *Pf*LDH was selectively separated (Fig. 1(A)). *Pf*LDH and hLDH were

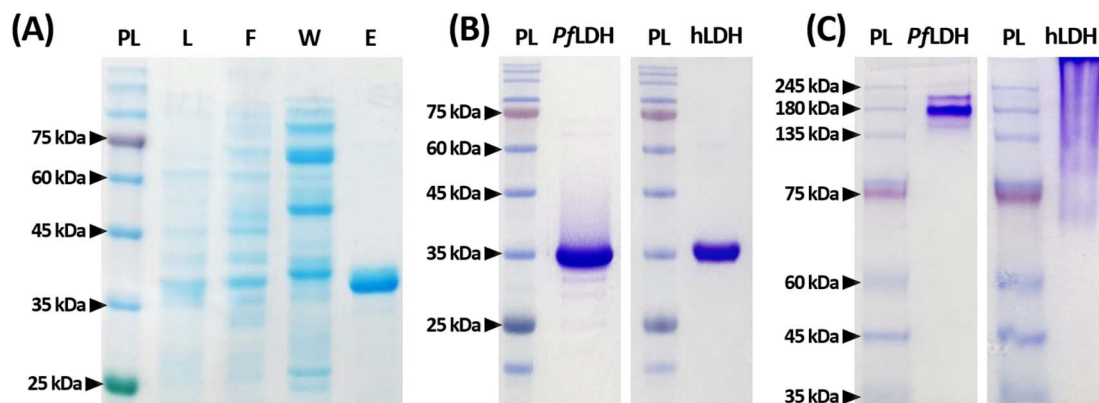


Fig. 1 Polyacrylamide gel electrophoresis for *Plasmodium falciparum* lactate dehydrogenase (*Pf*LDH) and human lactate dehydrogenase (hLDH) proteins. (A) A gel image of each immobilized metal affinity chromatography (IMAC) fraction. Electrophoresis was performed on a 12% polyacrylamide gel under reduced conditions. PL, protein ladder; L, lysate of *Escherichia coli* BL21(DE3) carrying plasmid pET-21a(+)-*Pf*LDH; F, flow-through fraction after initially loading the BL21(DE3) lysate onto a column packed with nickel-nitrilotriacetic acid agarose beads; W, the washing fraction from the IMAC procedure; E, the elution fraction from the IMAC procedure. (B) Gel images of purified *Pf*LDH (left) and purified hLDH (right). Electrophoresis was performed on a 15% polyacrylamide gel under reduced conditions. (C) Gel images of purified *Pf*LDH (left) and purified hLDH (right). Electrophoresis was performed on a 10% polyacrylamide gel under native (non-reduced) conditions.



highly purified in the reduced condition, as indicated by a single band on 15% polyacrylamide gels at approximately 36 kDa (Fig. 1(B)). In the native condition on 10% polyacrylamide gels, we observed bands above 140 kDa for both proteins, while no bands were observed around 36 kDa (Fig. 1(C)).

The *Pf*LDH and hLDH molecular weights do not match in the native condition due to differences in their isoelectric points (pIs). The *Pf*LDH and hLDH pIs are 7.26 and 8.64, respectively. In native gels, it is natural that hLDH migrates less than *Pf*LDH in a resolving gel with a pH of 8.8. On the other hand, since the protein ladder molecules are stored in a buffer containing 20 mM Tris-phosphate (pH 7.5), 2% SDS, 3.6 M urea, 0.2 mM dithiothreitol, and 15% glycerol, they are located in appropriate molecular weight. These results suggest that the *Pf*LDH and hLDH proteins used in this experiment were well-composed of tetramers.

Optimizing the reaction conditions and binding affinity measurements

Scheme 1 illustrates the proposed ELASA procedure for detecting *Pf*LDH. Prior to perform the ELASA, we examined the binding affinity between *Pf*LDH and the 2008s aptamer. The 2008s aptamer against *Pf*LDH was adopted by Cheung *et al.*, who performed a structural study that defined the *Pf*LDH binding site.²¹ Direct immobilization of the 2008s aptamer on a microwell plate may interrupt *Pf*LDH binding. Therefore, biotin was conjugated at the 3'-end of the aptamer sequence for flexible binding with *Pf*LDH. Also, the aptamer's primary binding sequence is at the 5'-end, and thus biotin was conjugated at the 3'-end.

First, we coated the microwell plates with 1 $\mu\text{g mL}^{-1}$ of streptavidin, then bound 10 nM of structured biotinylated *Pf*LDH aptamer through biotin-streptavidin pairing (Fig. 2(A)).

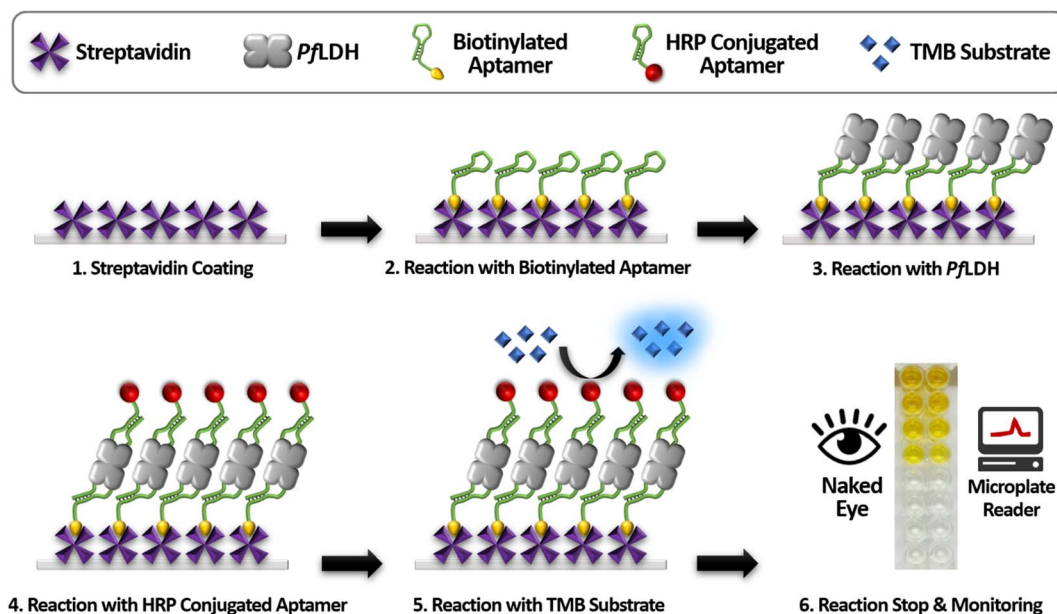
Next, the HRP-conjugated *Pf*LDH was serially diluted to different concentrations (0 to 2 μM) and incubated with the coated the 2008s aptamer. Here, we used three different buffer conditions to determine the best reaction: buffer A: PBS, pH 7.4, buffer B: 25 mM Tris-Cl (pH 7.5), 100 mM NaCl, and 20 mM imidazole, and buffer C: 10 mM Tris-Cl (pH 7.4), 10 mM NaCl, and 0.2 mM MgCl_2 . Each microwell was treated with TMB substrate to trigger a color reaction based on the HRP-conjugated *Pf*LDH remaining in the microwell, which was terminated with a 0.5 N H_2SO_4 solution. Finally, colorization was monitored by the naked eye, and the absorbance was measured at 450 nm using a microplate reader.

The dissociation constant (K_D) was calculated by extracting the absorbance from each *Pf*LDH concentration using the following equation:

$$\text{Abs} = \text{Abs}_{\text{min}} + \Delta\text{Abs} \times \left(\frac{[\text{PfLDH}]}{K_D + [\text{PfLDH}]} \right)$$

Abs, ΔAbs , and $[\text{PfLDH}]$ represent the measured absorbance, total change in absorbance, and molar concentration of *Pf*LDH, respectively. Similar K_D values were obtained from each reaction buffer (Fig. 2(B-D)). The K_D value of buffer A (PBS, pH 7.4) was 53.17 ± 2.97 nM, and the R^2 value was 0.9975, showing the least variation (Fig. 2(B)). The K_D values for buffers B and C were 33.81 ± 4.24 nM and 74.55 ± 4.76 nM, respectively (Fig. 2(C and D)), and the R^2 values were 0.9873 and 0.9968, respectively. These results indicate that any general buffer could be used for binding assays with this aptamer. Moreover, our K_D values aligned with those reported by Cheung *et al.*, determined by isothermal titration calorimetry ($K_D = 42$ nM) and an electrophoretic mobility shift assay ($K_D = 56$ nM).²¹

HRP-conjugated *Pf*LDH binding did not occur in the BSA-coated microwells without streptavidin (white circles in



Scheme 1 A schematic illustration of the enzyme-linked aptamer-based sandwich assay for detecting *Plasmodium falciparum* lactate dehydrogenase (*Pf*LDH). HRP, horseradish peroxidase; TMB, 3,3',5,5'-tetramethylbenzidine.



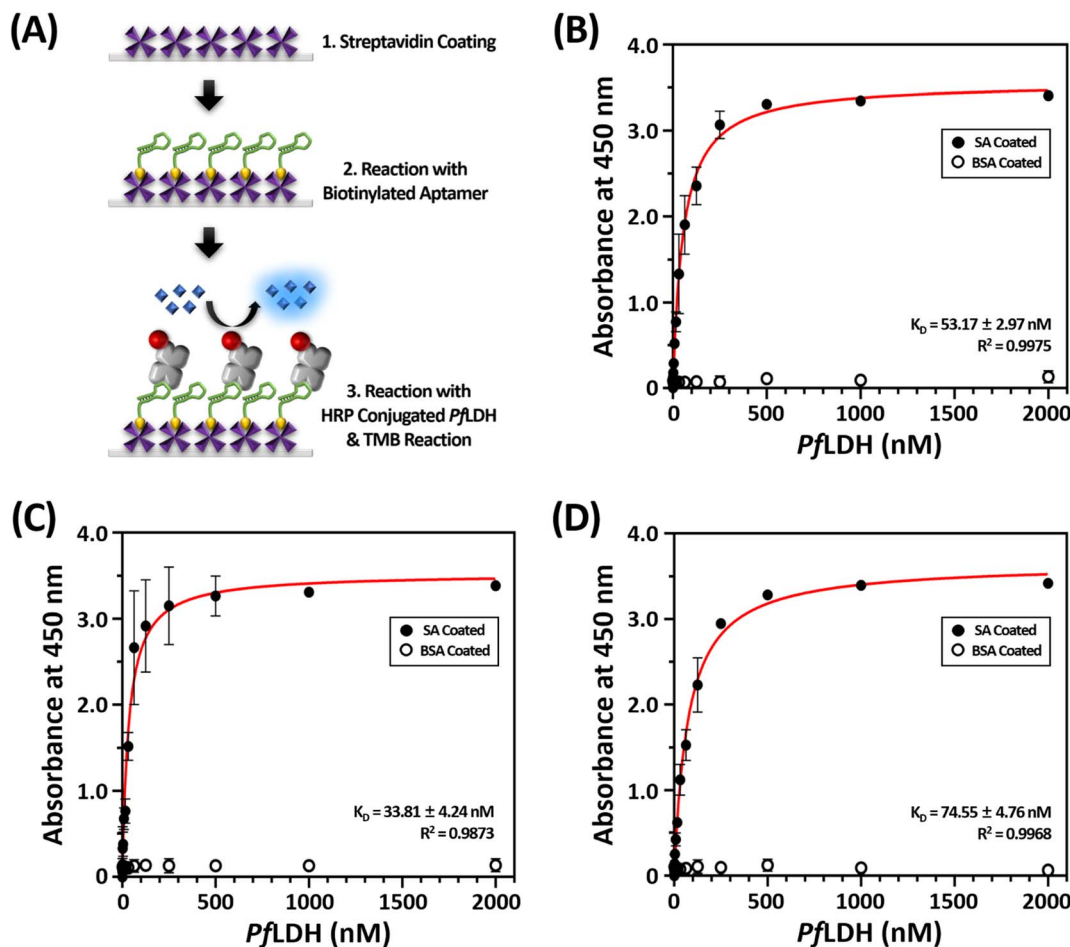


Fig. 2 The principle and the binding affinity results between *Plasmodium falciparum* lactate dehydrogenase (*PfLDH*) and the 2008s aptamer. (A) Schematic illustration of the experimental procedures for the dissociation constant (K_D) analysis between *PfLDH* and the 2008s aptamer. (B–D) *PfLDH* and the 2008s aptamer interaction binding curves using three different buffer conditions for the whole analysis procedures. Phosphate buffered saline (pH 7.4) was used in (B), 25 mM Tris–Cl (pH 7.5), 100 mM NaCl, and 20 mM imidazole was used in (C), and 10 mM Tris (pH 7.4), 10 mM NaCl, and 0.2 mM $MgCl_2$ was used in (D). The circles in (B) to (D) indicate streptavidin (SA, black circles) and bovine serum albumin (BSA, white circles) coated on microplates.

Fig. 2(B–D)), indicating that the absorbance increase with increasing *PfLDH* concentrations resulted from specific binding between *PfLDH* and the 2008s aptamer linked to streptavidin in the wells. Also, we examined the reaction between the 2008s aptamer and streptavidin as a negative control, which confirmed that the absorbance did not increase with increasing HRP-conjugated 2008s aptamer concentrations in the streptavidin-immobilized microwells (Fig. 3). Therefore, *PfLDH* and the 2008s aptamer bind specifically in a microwell plate.

PfLDH aptamer sensitivity in the ELASA platform

Next, we performed a *PfLDH* detection experiment using the ELASA method (Scheme 1). First, we saturated the microwells with 1 μM of streptavidin for efficient *PfLDH* molecule capture (*i.e.*, the coating step). Then, 1 μM of biotinylated aptamer was bound with the coated streptavidin through biotin–streptavidin pairing. Next, 100 $\mu g mL^{-1}$ of purified *PfLDH* was 10 \times serially diluted and then added to the wells to calculate the quantifiable range. Then, 1 μM of HRP-conjugated 2008s aptamer was

bound with the captured *PfLDH* in the microwells and subsequently treated with TMB substrate to trigger colorization (terminated with 0.5 N H_2SO_4 solution). Finally, absorbance was measured at 450 nm using a microplate reader.

We observed by the naked eye a significant color change at 100 $ng mL^{-1}$ of *PfLDH*. Furthermore, we determined the limit of detection (LOD) and limit of quantification (LOQ) based on the absorbances (Fig. 4). In general, the LOD is an absorbance value that is 3 \times higher than that of the blank (negative control), and the LOQ is the absorbance value 10 \times higher than that of the blank. We calculated the LOD and LOQ in buffer as 21.3 $ng mL^{-1}$ and 44.0 $ng mL^{-1}$, respectively, using the following equation:

$$Abs = Abs_{min} + \frac{Abs_{max} - Abs_{min}}{1 + 10^{(\log EC_{50} - x)/H}}$$

Abs, EC_{50} , and H represent the interested absorbance from the *PfLDH* concentration at x , the half maximal effective *PfLDH* concentration, and the hillslope, respectively. Usually, capture and probe molecules bound to the target molecule are screened in a sandwich assay, then the optimal pair is selected. Even though



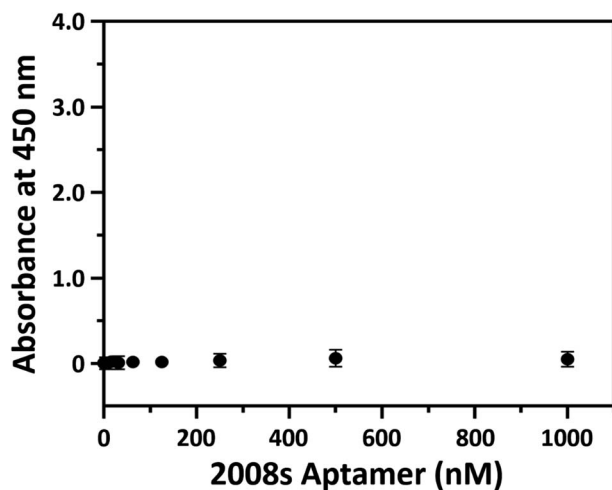


Fig. 3 Streptavidin and the 2008s aptamer binding. The x-axis represents the horseradish peroxidase (HRP)-conjugated 2008s aptamer concentration, and the y-axis represents the absorbance at 450 nm. A microwell plate was coated with $1 \mu\text{g mL}^{-1}$ of streptavidin, and then incubated with various HRP-conjugated 2008s aptamer concentrations (0 to 1000 nM).

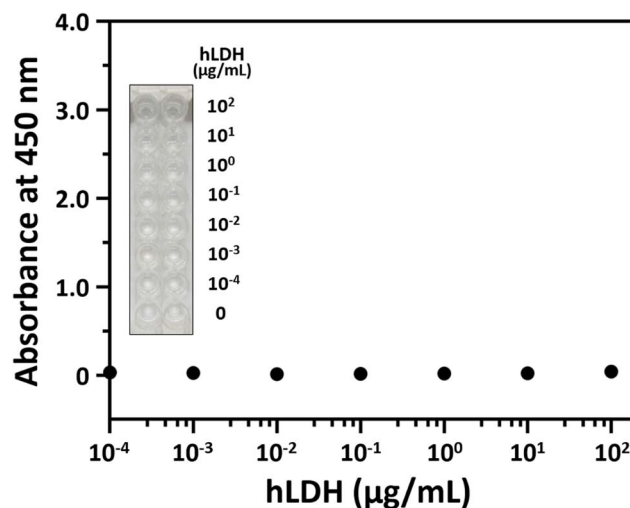


Fig. 5 Human lactate dehydrogenase (hLDH) detection with the enzyme-linked aptamer-based sandwich assay platform. The x-axis represents the hLDH concentrations ($0, 10^{-4}, 10^{-3}, 10^{-2}, 10^{-1}, 10^0, 10^1,$ and $10^2 \mu\text{g mL}^{-1}$), and the y-axis represents the absorbance at 450 nm. The inset image shows the color development after adding the color substrate but before adding the stop solution.

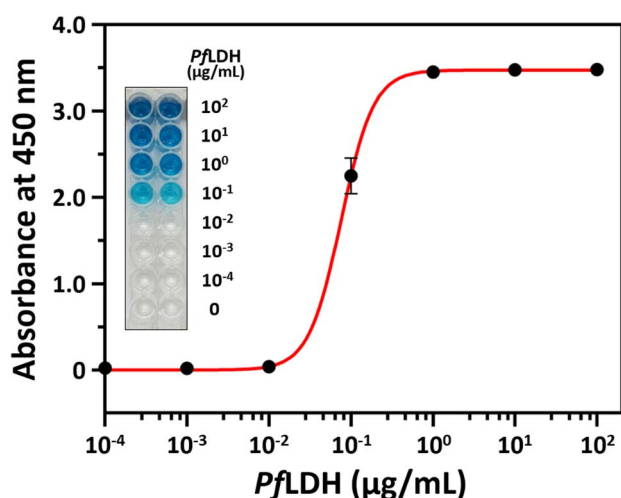


Fig. 4 *Plasmodium falciparum* lactate dehydrogenase (*PflDH*) detection with the enzyme-linked aptamer-based sandwich assay platform. The x-axis represents the *PflDH* concentrations ($0, 10^{-4}, 10^{-3}, 10^{-2}, 10^{-1}, 10^0, 10^1,$ and $10^2 \mu\text{g mL}^{-1}$), and the y-axis represents the absorbance at 450 nm. The inset image shows the color development after adding the color substrate but before adding the stop solution.

two different molecules optimized for capturing and probing the target molecule are used, our proposed ELASA method is distinct from conventional methods because the sandwich assay was performed using a single aptamer sequence with dual binding sites owing to the tetrameric characteristics of *PflDH*.

PflDH aptamer selectivity in the ELASA platform

The hLDH detection experiment was performed to examine the selectivity of our ELASA method using the 2008s aptamer. All

experimental conditions were adopted from the ELASA for *PflDH* detection, except that hLDH was used instead of *PflDH*. The hLDH was $10\times$ serially diluted from $100 \mu\text{g mL}^{-1}$ and measured by ELASA to confirm whether non-specific binding between hLDH and the 2008s aptamer exists. hLDH did not bind the 2008s aptamer, evidenced by similar absorbances between the blank and the $100 \mu\text{g mL}^{-1}$ concentration (Fig. 5).

Moreover, multiple sequence alignment was performed on *PflDH* and hLDH amino acids using UniProt (Fig. 6). Of the 332 amino acid positions, 89 amino acids existed at the same positions in aligned sequence (purple color in Fig. 6), and the homology between *PflDH* and hLDH was 26.8%. Furthermore, we marked the primary binding site of the 2008s aptamer in *PflDH* based on the information based by Cheung *et al.*,²¹ which confirmed a difference in the amino acids sequence of *PflDH* and hLDH (yellow color in Fig. 6). A molecule of the 2008s aptamer binds to two monomers of *PflDH* that form a tetramer. Specifically, the 2008s aptamer binds to Asp35, Ile36, and Lys84 to Asp90 of *PflDH* monomer, and binds to Lys44 and His232 of another *PflDH* monomer. This difference contributes to the structural stability of the 2008s aptamer-*PflDH* complex, which has a different charge and polarity than hLDH. Together, these results indicate that our ELASA selectively captures only *PflDH*, and thus it can be distinguished from hLDH in *P. falciparum*-infected blood samples for malaria diagnosis.

A quantitative analysis of *PflDH* in a blood sample using the ELASA platform

Finally, we performed an experiment to validate that *PflDH* can be selectively detected in the blood with high sensitivity. First, we spiked mouse blood with *PflDH* to final concentrations of $0, 10^{-4}, 10^{-3}, 10^{-2}, 10^{-1}, 10^0, 10^1,$ and $10^2 \mu\text{g mL}^{-1}$ of *PflDH*.



platform features make it an attractive option for clinical application. Using this ELASA platform may improve *P. falciparum* infection diagnosis and could be extended to other malaria parasites.

Author contributions

Conceptualization, J.-W. C.; data curation, Y.-J. K.; methodology, Y.-J. K. and J.-W. C.; resources, Y.-J. K. and J.-W. C.; formal analysis, J.-W. C.; visualization, Y.-J. K. and J.-W. C.; investigation, J.-W. C.; supervision, J.-W. C.; writing-original draft, Y.-J. K. and J.-W. C.; writing-review and editing, Y.-J. K. and J.-W. C.; funding acquisition, J.-W. C. Both authors have read and agreed to the published version of the manuscript.

Conflicts of interest

There are no conflicts to declare.

Acknowledgements

This work was supported by Regional Innovation Strategy (RIS) and Basic Research Program through the National Research Foundation (NRF) of Korea funded by the Ministry of Education (MOE) (No. 2021RIS-001) and Ministry of Science and ICT (MSIT) (No. 2021R1F1A1062994), respectively. This work was also supported by Bio-Convergence Technology Education Program through the Korea Institute for Advancement of Technology (KIAT) funded by the Ministry of Trade, Industry and Energy (MOTIE) (No. P0017805).

Notes and references

- 1 World Health Organization (WHO), *World Malaria Report 2021*, Geneva, 2021.
- 2 L. Neves Borgheti-Cardoso, M. San Anselmo, E. Lantero, A. Lancelot, J. L. Serrano, S. Hernández-Ainsa, X. Fernández-Busquets and T. Sierra, *J. Mater. Chem. B*, 2020, **8**, 9428–9448.
- 3 M. A. Phillips, J. N. Burrows, C. Manyando, R. H. van Huijsduijnen, W. C. Van Voorhis and T. N. C. Wells, *Nat. Rev. Dis. Primers*, 2017, **3**, 17050.
- 4 W. M. Fong Amaris, C. Martinez, L. J. Cortés-Cortés and D. R. Suárez, *Malar. J.*, 2022, **21**, 74.
- 5 P. U. Eze and C. O. Asogwa, *Bioengineering*, 2021, **8**, 150.
- 6 G. S. Alemayehu, K. Blackburn, K. Lopez, C. Cambel Dieng, E. Lo, D. Janies and L. Golassa, *Malar. J.*, 2021, **20**, 109.
- 7 T. Hänscheid and M. P. Grobusch, *Trends Parasitol.*, 2002, **18**, 395–398.
- 8 K. Kassegne, S. W. Fei, K. Ananou, K. S. Noussougnon, K. Komi Koukoura, E. M. Abe, X. K. Guo, J. H. Chen and X. N. Zhou, *Front. Microbiol.*, 2021, **12**, 732923.
- 9 K. van Bergen, T. Stuitje, R. Akkers, E. Vermeer, R. Castel and T. Mank, *Malar. J.*, 2021, **20**, 314.
- 10 C. Morang'a, C. Ayieko, G. Awinda, R. Achilla, C. Moseti, B. Ogutu, J. Waitumbi and E. Wanja, *Malar. J.*, 2018, **17**, 10.
- 11 M. L. Gatton, A. Chaudhry, J. Glenn, S. Wilson, Y. Ah, A. Kong, R. L. Ord, R. R. Rees-Channer, P. Chiodini, S. Incardona, Q. Cheng, M. Aidoo and J. Cunningham, *Malar. J.*, 2020, **19**, 392.
- 12 A. Badiane, J. Thwing, J. Williamson, E. Rogier, M. A. Diallo and D. Ndiaye, *Int. J. Infect. Dis.*, 2022, **121**, 92–97.
- 13 A. Calderaro, S. Montecchini, M. Buttrini, G. Piccolo, S. Rossi, M. C. Arcangeletti, B. Farina, F. De Conto and C. Chezzi, *Microorganisms*, 2021, **9**, 2265.
- 14 P. E. Brasil, L. De Castro, A. M. Hasslocher-Moreno, L. H. Sangenis and J. U. Braga, *BMC Infect. Dis.*, 2010, **10**, 337.
- 15 R. M. Lequin, *Clin. Chem.*, 2005, **51**, 2415–2418.
- 16 P. S. Atchade, C. Doderer-Lang, N. Chabi, S. Perrotey, T. Abdelrahman, C. D. Akpovi, L. Anani, A. Bigot, A. Sanni and E. Candolfi, *Malar. J.*, 2013, **12**, 279.
- 17 I. M. Ali, A. M. Nji, J. C. Bonkum, M. N. Moyeh, G. K. Carole, A. Efon, S. Dabou, V. P. K. Tchuensam, C. Tah, J. C. Kengne, D. F. Achu, J. D. Bigoga and W. F. Mbacham, *Diagnostics*, 2021, **11**, 1556.
- 18 Y. Lo, Y. W. Cheung, L. Wang, M. Lee, G. Figueroa-Miranda, S. Liang, D. Mayer and J. A. Tanner, *Biosens. Bioelectron.*, 2021, **192**, 113472.
- 19 N. S. Gopal and R. Raychaudhuri, *Malar. Res. Treat.*, 2017, **2017**, 9062514.
- 20 L. D. Kori, N. Valecha and A. R. Anvikar, *Sci. Rep.*, 2020, **10**, 6307.
- 21 Y. W. Cheung, J. Kwok, A. W. Law, R. M. Watt, M. Kotaka and J. A. Tanner, *Proc. Natl. Acad. Sci. U. S. A.*, 2013, **110**, 15967–15972.
- 22 J. D. Wirth, J. I. Boucher, J. R. Jacobowitz, S. Classen and D. L. Theobald, *Biochemistry*, 2018, **57**, 6434–6442.
- 23 S. Khrapunov, A. Waterman, R. Persaud and E. P. Chang, *Biochemistry*, 2021, **60**, 3582–3595.
- 24 L. P. Sousa, L. A. Mariuba, R. J. Holanda, J. P. Pimentel, M. E. Almeida, Y. O. Chaves, D. Borges, E. Lima, J. L. Crainey, P. P. Orlandi, M. V. Lacerda and P. A. Nogueira, *BMC Infect. Dis.*, 2014, **14**, 49.
- 25 S. Lee, K. M. Song, W. Jeon, H. Jo, Y. B. Shim and C. Ban, *Biosens. Bioelectron.*, 2012, **35**, 291–296.
- 26 K. A. Frith, R. Fogel, J. P. D. Goldring, R. G. E. Krause, M. Khati, H. Hoppe, M. E. Cromhout, M. Jiwaji and J. L. Limson, *Malar. J.*, 2018, **17**, 191.
- 27 R. M. Dirkzwager, A. B. Kinghorn, J. S. Richards and J. A. Tanner, *Chem. Commun.*, 2015, **51**, 4697–4700.
- 28 Y. W. Cheung, R. M. Dirkzwager, W. C. Wong, J. Cardoso, J. D'Arc Neves Costa and J. A. Tanner, *Biochimie*, 2018, **145**, 131–136.
- 29 G. Figueroa-Miranda, Y. Liang, M. Suranglikar, M. Stadler, N. Samane, M. Tintelott, Y. Lo, J. A. Tanner, X. T. Vu, J. Knoch, S. Ingebrandt, A. Offenhäusser, V. Pachauri and D. Mayer, *Biosens. Bioelectron.*, 2022, **208**, 114219.
- 30 M. M. Plucinski, P. D. McElroy, P. R. Dimbu, F. Fortes, D. Nace, E. S. Halsey and E. Rogier, *Parasites Vectors*, 2019, **12**, 293.
- 31 D. J. Bzik, B. A. Fox and K. Gonyer, *Mol. Biochem. Parasitol.*, 1993, **59**, 155–166.
- 32 L. Vivas, A. Easton, H. Kendrick, A. Cameron, J. L. Lavandera, D. Barros, F. G. de las Heras, R. L. Brady and S. L. Croft, *Exp. Parasitol.*, 2005, **111**, 105–114.

